Effect of a built-in electric field in asymmetric ferroelectric tunnel junctions

Yang Liu,[1,2,*] Xiaojie Lou,[1] Manuel Bibes,[3] and Brahim Dkhil[2]

[1]*Multi-disciplinary Materials Research Center, Frontier Institute of Science and Technology, Xi'an Jiaotong University, Xi'an 710054, People's Republic of China*

[2]*Laboratoire Structures, Propriétés et Modélisation des Solides, UMR 8580 CNRS-Ecole Centrale Paris, Grande Voie des Vignes, 92295 Châtenay-Malabry Cedex, France*

[3]*Unité Mixte de Physique CNRS/Thales, 1 Av. A. Fresnel, Campus de l'Ecole Polytechnique, 91767 Palaiseau and Université Paris-Sud, 91405 Orsay, France*

(Received 6 October 2012; revised manuscript received 3 May 2013; published 11 July 2013)

The contribution of a built-in electric field to ferroelectric phase transition in asymmetric ferroelectric tunnel junctions is studied using a multiscale thermodynamic model. It is demonstrated in detail that there exists a critical thickness at which an unusual ferroelectric-"polar nonferroelectric" phase transition occurs in asymmetric ferroelectric tunnel junctions. In the "polar nonferroelectric" phase, there is only one nonswitchable polarization which is caused by the competition between the depolarizing field and the built-in field, and closurelike domains are proposed to form so as to minimize the system energy. The transition temperature is found to decrease monotonically as the ferroelectric barrier thickness is decreased and the reduction becomes more significant for the thinner ferroelectric layers. As a matter of fact, the built-in electric field not only results in smearing of the phase transition, but also forces the transition to take place at a reduced temperature. Such findings may impose a fundamental limit on the work temperature and thus should be further taken into account in the future ferroelectric-tunnel-junction–type or ferroelectric-capacitor–type devices.

DOI: 10.1103/PhysRevB.88.024106 PACS number(s): 77.80.B−, 77.22.Ej, 77.80.−e

I. INTRODUCTION

Ferroelectric (FE) tunnel junctions (FTJs) that are composed of FE thin films of a few unit cells sandwiched between two electrodes (in most cases the top and bottom electrodes are different) have attracted much more attention during the last decade.[1–3] It is generally believed that the interplay between ferroelectricity and quantum-mechanical tunneling plays a key role in determining tunnel electroresistance (TER) or tunneling current, and the TER effect usually takes place upon polarization reversal. Due to the strong coupling of FE polarization and the applied field, the electric-field control of TER or tunneling current,[1–11] spin polarization,[12–26] and electrocaloric effect[27] can be achieved, which makes FEs promising candidates for nondestructive FE storage,[1–10] FE memristor,[11] spintronics (magnetization),[12–26] or electrocaloric[27] devices. Meanwhile, another mechanically (including strain or strain gradient) induced TER is found recently, which also shows its potential applications in mechanical sensors, transducers, and low-energy archive data storage devices.[28] Note that having different electrodes for the FTJs (some experiments use conductive atomic force microscope tips instead of the top electrodes) is usually required for a large effect at low-bias voltage, although the FTJs with the same electrodes may also display interesting performances.[2,4,9,18] Also note that all the functionalities in these devices are strongly related to the thermodynamic stability and switching ability of FTJs.[1–28] Therefore, a fundamental understanding of ferroelectricity of FTJs, especially their size effects, is crucial at the current stage of research.

Unfortunately, no consensus has been achieved on whether there exists a critical thickness h_c below which the ferroelectricity disappears in FTJs, especially for those with different top and bottom electrodes. It is believed that an electrostatic depolarizing field caused by dipoles at the FE-metal interfaces is responsible for the size effect.[29–34] However, recent theoretical studies suggest that the choice of electrode material may lead to smearing of size effect or even vanishing of h_c.[35–39] For example, it was reported that choosing Pt as electrodes would induce a strong interfacial enhancement of the ferroelectricity in Pt/$BaTiO_3$(BTO)/Pt FTJs, where h_c is only an 0.08 BTO unit cell.[35] In addition, the results of a modified thermodynamic model[36,37] and first-principles calculations[38,39] both indicate that the BTO barrier with dissimilar electrodes, i.e., Pt and $SrRuO_3$ (SRO) electrodes, might be free of deleterious size effects. In contrast, it has been reported that asymmetric combination of the electrodes (including the same electrodes with different terminations) will result in the destabilization of one polarization state making the asymmetric FTJs non-FE.[33,40] And, the up-to-date studies reported that the fixed interface dipoles near the FE/electrode interface is considered the main reason for that detrimental effect.[41,42] Considering the importance of the physics in FTJs with dissimilar top and bottom electrodes, we are strongly motivated to investigate the size effect in such asymmetric FTJs.

It was pointed out as early as 1963 that the contribution of different electronic and chemical environments of the asymmetric electrode/FE interfaces would induce a large long-range electrostatic built-in electric field $\vec{E}_{bi}$ in FE thin films.[43] $\vec{E}_{bi}$ becomes more significant in asymmetric FTJs and should be taken into account.[33,34] In this study, we use a multiscale thermodynamic model[27,33,34] to investigate the effect of such built-in electric field on the phase transition of asymmetric FTJs by neglecting the short-range interface dipoles. As a result, we discover an unusual FE-"polar non-FE" phase transition in asymmetric FTJs. Then, we make a detailed analysis of the contribution of the built-in electric field to FE phase transition, i.e., h_c, what happens below h_c, transition temperature T_c, and temperature dependence of dielectric response of the asymmetric FTJs.

II. MULTISCALE THERMODYNAMIC MODEL FOR THE FTJs

We concentrate on a short-circuited (001) single-domain FE plate of thickness h sandwiched between different electrodes. The FE films are fully strained and grown on thick (001) substrate with the polar axis lying normal to the FE-electrode interfaces.[32–34] We denote the two interfaces as 1 and 2, with surface normals $\vec{n}_1$ and $\vec{n}_2 = -\vec{n}_1$ pointing into the electrodes. The configurations are schematically shown in Fig. 1. The exact value and direction of $\vec{E}_{bi}$ can be determined as[33,34]

$$\vec{E}_{bi} = -\frac{\Delta\varphi_2 - \Delta\varphi_1}{h}\vec{n} = -\frac{\delta\varphi}{h}\vec{n} \text{ and } \vec{n} = \vec{n}_2 = -\vec{n}_1, \quad (1)$$

where $\Delta\varphi_i$, which is the work function steps for the FE-electrode i interface at zero polarization, is simply defined as the potential difference between the FE and the electrode i.[33,34] With the help of first-principles calculations, one could easily obtain $\Delta\varphi_i$ through the analysis of the electrostatic potential of FTJs where FE films are in the paraelectric (PE) state.[33,34]

Then, the free energy per unit surface of the FE layer is written as[33,34]

$$F = h\Phi + \Phi_S = \left(\frac{1}{2}\alpha_1^* P^2 + \frac{1}{4}\alpha_{11}^* P^4 + \frac{1}{6}\alpha_{111}P^6 + \frac{1}{8}\alpha_{1111}P^8 + \frac{u_m^2}{S_{11}+S_{12}} - \frac{1}{2}\vec{E}_{\text{dep}}\cdot\vec{P} - \vec{E}_{bi}\cdot\vec{P} - \vec{E}\cdot\vec{P}\right)h + (\zeta_1 - \zeta_2)\vec{n}\cdot\vec{P} + \frac{1}{2}(\eta_1+\eta_2)P^2, \quad (2)$$

where α_i^* are Landau coefficients.[27] u_m is the epitaxial strain and S_{mn} are the elastic compliance coefficients. ζ_i and η_i are the first- and second-order coefficients of the surface energy Φ_S expansion for the two FE-electrode interfaces.[33,34] $\vec{E}$ is the applied electric field along the polar axis. $\vec{E}_{\text{dep}}$ is the depolarizing field which can be determined from the short-circuit condition such that[33,34]

$$\vec{E}_{\text{dep}} = -\frac{\lambda_1 + \lambda_2}{h\varepsilon_0 + (\lambda_1+\lambda_2)\varepsilon_b}\vec{P}, \quad (3)$$

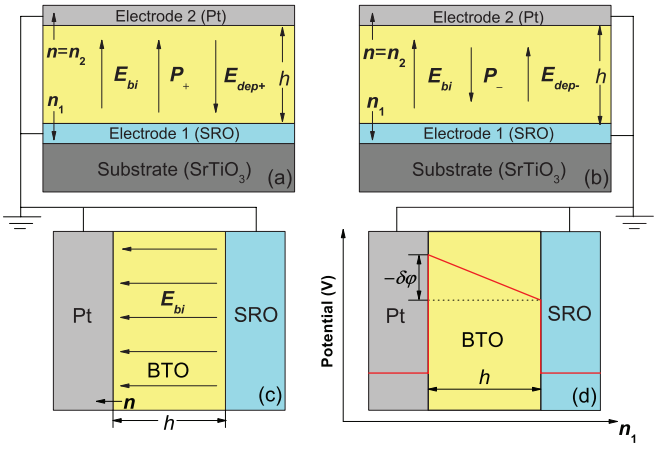

FIG. 1. (Color online) Schematic configurations of the system considered in the present calculations for the the asymmetric FTJs: P_+ state (a); P_- state (b); $\vec{E}_{bi}$ (c) and the corresponding potential profile at zero polarization (red line) (d).

where ε_0 is the permittivity of vacuum space, and ε_b indicates the background (i.e., without contribution of the spontaneous polarization) dielectric constant. λ_i are the effective screening lengths of the two interfaces and are dependent on the polarization direction if the electronic and chemical environments of FE/electrode interfaces are different.[33,34] For the two opposite polarization orientations, the direction dependence of λ_i will induce the asymmetry in potential energy and hence will produce the TER effect, besides the depolarizing field effect due to the polarization difference between two opposite orientations.[1–3] However, we ignore such an effect due to the lack of information about the direction dependence of λ_i and we mainly focus on the role of the built-in field in this study. Note that $\delta\varphi$ and $\delta\zeta = (\zeta_2 - \zeta_1)$ are thickness and polarization independent and $\vec{E}_{bi}$ is indeed a long-range internal-bias field which has the effect of poling the FE film.[33,34,43] In asymmetric FTJs, such asymmetry parameters $\delta\varphi$ and $\delta\zeta$ can introduce a potential energy profile difference and therefore induce the TER effect.[1–3]

The equilibrium polarization can be derived from the condition of thermodynamic equilibrium:

$$\frac{\partial F}{\partial P} = 0. \quad (4)$$

The dielectric constant ε under an applied field E whose direction is along the polar axis can be determined as[37]

$$\varepsilon = \frac{1}{h\varepsilon_0}\left(\frac{\partial^2 F}{\partial^2 P}\right)^{-1}. \quad (5)$$

The multiscale thermodynamic model used in this study combines first-principles calculations and phenomenological theory and its detailed description can be found elsewhere.[33,34] In a previous study, it is reported that $\vec{E}_{bi}$ could result in a smearing of the phase transition and an internal-bias-induced piezoelectric response above T_c in asymmetric FTJs.[33] However, adding to the foregoing controversy on the size effects, further analysis of the effect of a built-in field on the FE transition in asymmetric FTJs is still absent. Inserting Eq. (1) into (2) results in a term that encompasses an odd power of the polarization $\vec{E}_{bi}\cdot\vec{P}$, which leads to asymmetric thermodynamic potentials. We shall show that this term which behaves mathematically as identically as the phenomenological term suggested by Bratkovsky and Levanyuk[44] will result in an unusual FE-"polar non-FE" phase transition in asymmetric FTJs.

III. RESULTS AND DISCUSSION

A. Size effects

For a quantitative analysis, we consider a fully strained BTO film sandwiched between Pt (electrode 2) and SRO (electrode 1) epitaxially grown on (001) $SrTiO_3$ substrates. We neglect the energy difference of the asymmetric surfaces, i.e., by setting $\zeta_1 = \zeta_2$, $\eta_1 = \eta_2$, to ensure that the effect of $\vec{E}_{bi}$ is clearly observable from the calculations since it is reported that surface effects are generally much smaller than that of $\vec{E}_{bi}$.[36,37] All the parameters we used are listed in Ref. 65. We first examine the effect of $\vec{E}_{bi}$ on the ferroelectricity of asymmetric FTJs. Previous studies indicate that the direction

of $\vec{E}_{bi}$ in asymmetric Pt/BTO/SRO FTJs points to a Pt electrode with higher work function.[36–38] All recent results show indeed that a strong preference for one polarization state, namely P_+, while P_- disappears at "h_c." [36–42] According to the definition of ferroelectricity, the spontaneous polarization of the FE materials is switchable under an ac electric field.[45] However, knowing that the spontaneous polarization of FE materials is switchable under an ac electric field,[45] recent reports[36–39] are rather confusing and remain incomplete on this point. Indeed, in addition to the aforementioned divergence in the size effects, two different transition temperatures at which the two polarization states reach zero are obtained (see Ref. 37), which may be confusing since there should be only one finite phase transition temperature for disappearance of ferroelectricity. In order to avoid such confusions, we used the classical definition of ferroelectricity[45] in the following parts.

We make further analysis of the physical formulation of h_c in asymmetric FTJs. Note that Eq. (4) is a nonlinear equation and yields "at most" three solutions P, two of them corresponding to minima and the other one to a saddle point (unstable state). Whether the solution is a minimum, a maximum, or a saddle point can be revealed through inspecting the eigenvalues of the Hessian matrix of the total free energy F. Because the asymmetric FTJ is internally biased, i.e., the energy degeneracy between positive P_+ and negative P_- is lifted, one of the minima corresponds to the equilibrium state (the global minimum) of the system (the direction of which is along $\vec{E}_{bi}$) and the other minima corresponds to a metastable state (a local minimum) of the system. It means that the presence of two different electrodes in asymmetric FTJs results in a preferred polarization orientation of the FE plate. Having found all P solutions as a function of h, one can clearly see that metastable state and unstable state solutions become closer to each other and coincide at finite h, henceforth the number of solutions P drops from three to one. According to the bistable property of FE materials, this finite h is just h_c.[45] As long as there are three P solutions, two of these three solutions correspond to stable/metastable polarizations so that two orientations of polarization are possible in the BTO layer and thus it is FE. Switching the asymmetric FTJ into its unfavored high-energy polarization may be difficult. If there is the only P solution corresponding to the unstable state, although it attains a finite value, it is not FE anymore and may be called "PE." Indeed, it would be more appropriate to consider it as "polar non-FE" since P has a unique finite value.[46–48] FTJs with no built-in field $\delta\varphi = 0$ will exhibit two energetically equivalent stable polarization states (P_+ and P_-) along with an unstable polarization state at $P = 0$ below h_c. All the foregoing discussions can be clearly and easily understood in the schematic representation of $F - P$ curves with different BTO thicknesses as shown in Fig. 2, which is quite similar with the results of FE thin films with/without consideration of the fixed interface dipoles near the asymmetric FE/electrode interface[40–42] or FE superlattices with/without interfacial space charges.[48] Together with previous results,[41,42] we conclude that whether the $\vec{E}_{bi}$ is considered as a long-range field or a short-range surface one, it can not induce the vanishing of h_c in asymmetric FTJs, which is in contrast with other works.[36–39]

Note that the "polar non-FE" phase is actually a pyroelectric phase because there is a nonswitchable polarization

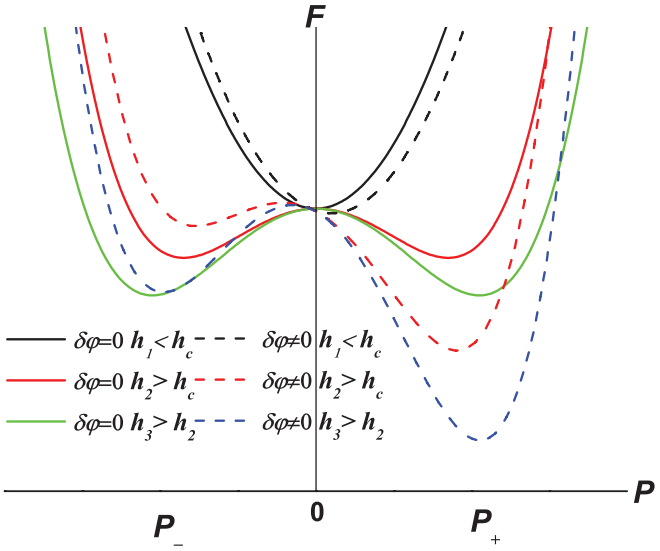

FIG. 2. (Color online) Schematic representation of the variation in total free energy with respect to polarization with different BTO barrier thicknesses in asymmetric Pt/BTO/SRO tunnel junctions with/without consideration of the built-in field in zero applied field.

in this phase. This kind of phase transition has once been reported in FE thin films with asymmetric electrodes[33,40–42] or FE superlattices with interfacial space charge.[46–48] As we discussed in the formation of h_c, the "polar non-FE" phase indeed always corresponds to the unstable state (see Fig. 2) and this kind of nonswitchable polarization may not be stable at all. However, breaking up the system into 180° domain stripes is unambiguously ruled out due to the long-range pinned field $\vec{E}_{bi}$. In-plane vortex formation[50,51] is also inhibited because the large compressive strain favors more 180° domain stripes.[51] The ferromagneticlike closure domains are predicted to form in ultrathin FE films or FE capacitors even below h_c (Refs. 52–54) and are experimentally confirmed well above h_c recently.[55,56] However, typical FE closure domains[52–56] are also not expected in the "polar non-FE" phase where 180° domains in the closure domain structure should be suppressed. But, local rotations of nonswitchable polarization (<90°) are still likely to occur and result in a closurelike domain structure since the local change of the direction of the nonswitchable polarization especially near the FE/electrode interface is helpful to minimize the system energy.[52–54] Although such closurelike domains can be favored below h_c (<3 nm at least), it is clear that the FE barrier as a whole is not FE according to our foregoing analysis that shows the polarization is not switchable under external electric fields. While a detailed analysis of the built-in field effect on domain formation is beyond the scope of this study, we suggest that more rigorous simulations should be made in the future. It can be seen that the asymmetric FTJs below h_c can not be used for FE memory applications in which two thermodynamic stable polarization states are needed to encode "0" and "1" in Boolean algebra.[29–34,45] However, based on our calculation, one should expect a resistance change below h_c between the nonswitchable polarization state and the other one being ferroelectrically dead. This result agrees well with recent works on Pt/BTO/Pt FTJs that even below

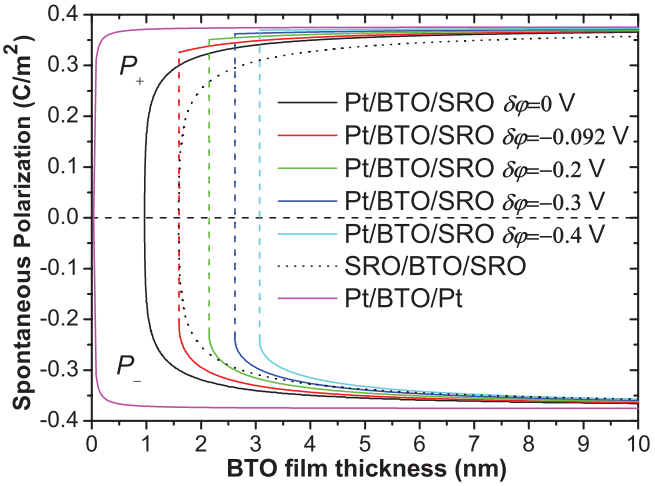

FIG. 3. (Color online) Spontaneous polarization of the asymmetric Pt/BTO/SRO tunnel junctions as a function of BTO layer thickness with $\delta\varphi = 0, -0.092, -0.2, -0.3$, and 0.4 V in zero applied field at 0 K, respectively. The results of symmetric SRO/BTO/SRO and Pt/BTO/Pt tunnel junctions at 0 K (Ref. 27) are also added for comparison.

h_c, the resistance of the FTJ would change by a factor of 3 due to the interface bonding and barrier decay rate effects.[4] We argue that the TER effect below h_c suggested in our work may be essentially attributed to the asymmetric modification of the potential barrier by the nonzero barrier height $(-\delta\varphi)$ [see Eqs. (1)–(4)] which even exists at zero polarization as shown in Fig. 1(d). Further theoretical and experimental efforts should be made to confirm these predictions.

The quantitative results of the foregoing analysis are directly given in Fig. 3. It can be seen that h_c exists regardless of symmetric or asymmetric structures. As expected, the curves of P_+ and P_- are symmetric with respect to $P = 0$ at $\delta\varphi = 0$ where h_c is about 1 nm, which is smaller than that of SRO/BTO/SRO, i.e., 1.6 nm.[27,35] When $\delta\varphi \neq 0$, the supposed degeneracy between P_+ and P_- occurs, i.e., P_+ is enhanced while P_- is reduced so the coordinate of the center of the hysteresis loop along the polarization axis $[1/2(P_+ + P_-)]$ is shifted along the direction of P_+. It is shown that such a displacement of the hysteresis loop along the polarization axis becomes more significant as the strength of $\vec{E}_{bi}$ increases. It may be attributed to the imprint caused by $\vec{E}_{bi}$ such that the whole shape of the hysteresis loop will shift along the direction of the field axis which is antiparallel to the direction of $\vec{E}_{bi}$.[45] Besides, it is found that as $\delta\varphi$ increases, h_c increases, which indicates that $\vec{E}_{bi}$ can enhance the size of h_c. Thus, whether h_c of the Pt/BTO/SRO junction is larger or smaller than that in the SRO/BTO/SRO counterpart strongly depends on the exact value of $\delta\varphi$ as shown in Fig. 3.

For the symmetric structures (SRO/BTO/SRO and Pt/BTO/Pt FTJs), one can easily see in Fig. 3 that the single domain in the FE layer destabilizes as the film thickness is decreased due to the depolarizing field effect.[27,29–34] And, it is shown in Fig. 3 that Pt/BTO/Pt FTJ whose h_c is merely an 0.08 BTO unit cell is nearly free of deleterious size effects,[27] which agrees well with the result of first-principles calculations.[35] h_c of SRO/BTO/SRO FTJ is about four BTO unit cells, which is well consistent with our previous results.[27] The qualitative result that h_c of Pt/BTO/Pt FTJ is smaller than that of SRO/BTO/SRO FTJ in this work is well consistent with those of first-principles calculations[35] and the lattice model.[57] However, our results are in contrast with previous works[31,36,37] predicting h_c of SRO/BTO/SRO FTJ to be smaller than that of Pt/BTO/Pt FTJ. In these previous works,[36,37] the Mehta *et al.* electrostatic theory about the depolarizing field $[\vec{E}_{\rm dep} = -\frac{\vec{P}}{\varepsilon_b}(1 - \frac{h/\varepsilon_b}{l_{s1}/\varepsilon_{e1}+l_{s2}/\varepsilon_{e2}+h/\varepsilon_b})$ where l_{s1} and l_{s2} are Thomas-Fermi screening lengths and ε_{e1} and ε_{e2} are dielectric constants of electrodes 1 and 2] is used,[29] while in our work we used the "effective screening length" model to describe the depolarizing field [see Eq. (3)]. Note that we used the same parameters as Refs. 36 and 37 except for the model of depolarizing field.[65] The distinct results are understandable since it is generally accepted that imperfect screening should be characterized by effective screening length [see Eq. (3)] rather than Thomas-Fermi one in the Mehta *et al.* model.[49] In fact, the effective screening length at Pt/BTO interface is only 0.03 Å,[35] much smaller than that of the Thomas-Fermi one ~0.4 Å,[31] so a significantly reduced depolarizing field is expected and it would result in nearly no h_c in Pt/BTO/Pt FTJs. A previous study attributes this freedom of size effects in the Pt/BTO/Pt structure to the "negative dead layer" near the Pt/BTO interface,[35] while we argue that it may result directly from the fact that the effective screening length of the Pt electrode is extremely small since Bratkovsky and Levanyuk suggested the "dead layer" model is totally equivalent as to consider an electrode with a finite screening length.[58] Here, we ignore the effect of the extrinsic "dead layer" formed between a metal electrode (i.e., Au or Pt) and a perovskite FE [i.e., $Pb(ZrTi)O_3$ or BTO]. Indeed, Lou and Wang found that the "dead layer" between Pt and $Pb(ZrTi)O_3$ is extrinsic and could be removed almost completely by doping 2% Mn.[59] Experimentally, many researchers found that SRO/BTO/SRO capacitors (as well as other perovskite FE structures with conductive oxide electrodes) are free from passive layers.[31,60,61] Recently, a very interesting experimental result demonstrates that the RuO_2/BaO terminations at BTO/SRO interface, which is assumed as many pinned interface dipoles and plays a detrimental role in stabilizing a switchable FE polarization, can be overcome by depositing a very thin layer of $SrTiO_3$ between the BTO layer and SRO electrode.[41,42] Nonetheless, it is still unclear whether such pinned interface dipoles are intrinsic and can be found in other FE/electrode interfaces (i.e., SRO/$PbTiO_3$ and Pt/BTO).

In the asymmetric structures in Fig. 3, it is shown that in comparison with $\delta\varphi = 0$ in asymmetric Pt/BTO/SRO FTJs, h_c is significantly enhanced, as $\delta\varphi$ increases, which is in good agreement with the recent results regarding $\vec{E}_{bi}$ as short-range interface field,[41] and is similar with the previous results.[37] Note that $\delta\varphi$ is intrinsic and determined strictly by the electronic and chemical environments of FE/electrode interfaces but not by any potential drop through the FTJ which "creates" an applied field.[33,34,43,44] Changing $\delta\varphi$ is simply due to the lack of its exact value and for the purpose of studying the effect of $\vec{E}_{bi}$ in asymmetric FTJs, which is similar to the previous method.[36,37] This method[36,37] indeed does not mean that any asymmetric electrodes are considered here since the electrode is replaced,

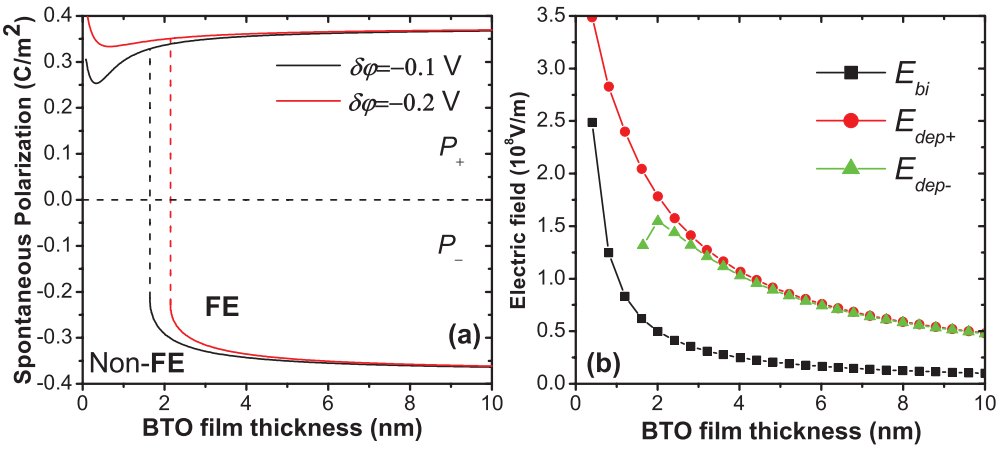

FIG. 4. (Color online) (a) Polarization state P_+ of the asymmetric Pt/BTO/SRO tunnel junctions as a function of BTO layer thickness with $\delta\varphi = -0.1$ and -0.2 V in zero applied field at 0 K, respectively. The dashed lines mark the boundary between polar non-FE and FE phases for different values of $\delta\varphi$. (b) Dependence of the strengths of the built-in field E_{bi} and depolarizing field for different directions $E_{\text{dep}+}$ and $E_{\text{dep}-}$ on the BTO layer thickness with $\delta\varphi = -0.1$ V at 0 K.

the electrode/FE interface parameters in Eqs. (1)–(3) such as λ_i and other interface parameters will also change. The variation of P_+ in Pt/BTO/SRO FTJs as a function of the whole BTO layer thickness with $\delta\varphi = -0.1$ and -0.2 V at 0 K is shown in Fig. 4(a). It is found that below the critical thickness, the P_+ state shows an interesting recovery of a polar non-FE polarization, in contrast to the P_- state [see Fig. 4(a)], becoming less significant when $\delta\varphi \sim< -0.2$ V. Note that such recovery has been reported in FE superlattices with asymmetric electrodes and demonstrated to be independent of the interfacial space charge.[46] Although such a recovery of polar non-FE polarization in the BTO layer does not mean the recovery of ferroelectricity as it is not switchable, it is necessary to realize its origin. We plot the built-in field E_{bi} and depolarizing field for different directions $E_{\text{dep}+}$ and $E_{\text{dep}-}$ as a function of the BTO film thickness considering $\delta\varphi = -0.1$ V as an example in Fig. 4(b). For the condition of the P_- state as schematically illustrated in Fig. 1(b), $E_{\text{dep}-}$ shows the typical behavior as the FTJ with the same electrodes,[30–32,57] which means that $E_{\text{dep}-}$ plays a key role forcing the single domain in the FE layer to destabilize as the film thickness is decreased. E_{bi} with the same direction of $E_{\text{dep}-}$ helps then to speed up such destabilization, therefore enhancing the critical thickness. For the P_+ state, $E_{\text{dep}+}$ and E_{bi} are in the opposite directions, as depicted in Fig. 1(a), and both the strengths of $E_{\text{dep}+}$ and E_{bi} increase as the BTO layer thickness is decreased [Fig. 4(b)], which means that $E_{\text{dep}+}$ is partially canceled by E_{bi}. The strength of this partial compensation becomes stronger with the film thickness decreasing (see the slopes of $E_{bi} - h$ and $E_{\text{dep}+} - h$ curves) [Fig. 4(b)]. Therefore, E_{bi} is fighting against $E_{\text{dep}+}$ allowing the polarization to recover into a polar non-FE polarization. This recovery of polar non-FE polarization forces the system to a higher-energy state which strongly supports our foregoing predictions of local rotations of nonswitchable polarization ($<90°$) and the formation of closurelike domain structure to minimize the system energy.

The critical thickness h_c under different ambient temperatures T as a function of $(-\delta\varphi)$ in asymmetric Pt/BTO/SRO FTJs is shown in Fig. 5. It can be seen that h_c decreases with T increasing. And it is found that for other T, the asymmetric Pt/BTO/SRO FTJs show a similar behavior of enhancement of h_c by increasing the strength of $\vec{E}_{bi}$ as shown in Fig. 3 at 0 K.

B. Transition temperature and dielectric response

The transition temperature T_c of the asymmetric FTJs is extremely important, especially for the device applications. Figure 6 summarizes T_c as a function of BTO thickness in epitaxial asymmetric Pt/BTO/SRO FTJs at various values of $\delta\varphi$. It is shown that T_c in asymmetric Pt/BTO/SRO FTJs monotonically decreases with the BTO layer thickness decreasing, which is similar to the behavior of symmetric SRO/BTO/SRO or Pt/BTO/Pt FTJs.[27] Moreover, T_c decreases more significantly for thinner BTO barrier layer thickness (see the slope of $T_c - h$ curves in Fig. 6). At a given BTO layer thickness, it is found in Fig. 7 that T_c decreases as $\delta\varphi$ becomes more negative, which means a larger built-in field can force the phase transition to occur at lower temperatures.

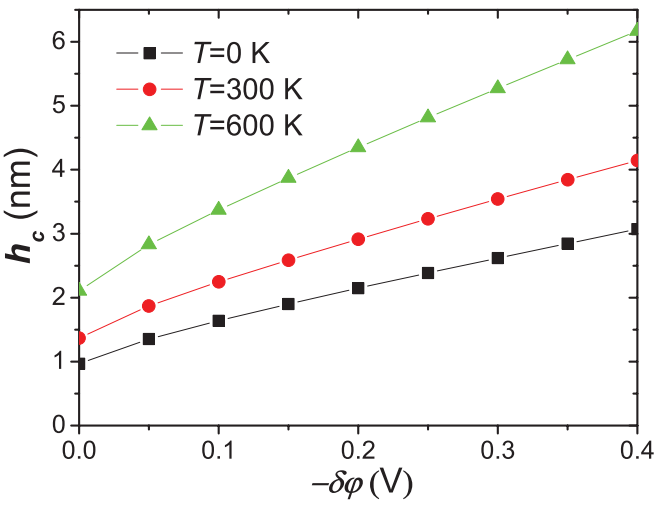

FIG. 5. (Color online) The variation in critical thickness h_c in epitaxial asymmetric Pt/BTO/SRO tunnel junctions as a function of $-\delta\varphi$ at three different temperatures: 0, 300, and 600 K, respectively ($E = 0$ kV/cm).

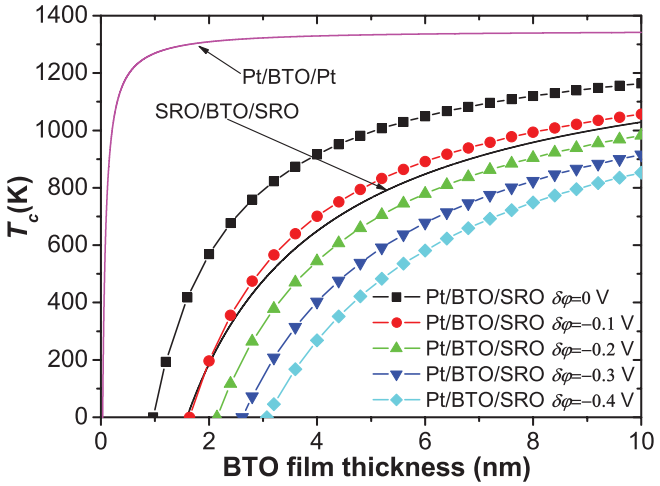

FIG. 6. (Color online) The transition temperature T_c as a function of BTO layer thickness in epitaxial asymmetric Pt/BTO/SRO tunnel junctions at various values of $\delta\varphi$ with no applied field. The results of symmetric SRO/BTO/SRO and Pt/BTO/Pt tunnel junctions (Ref. 27) are also provided for comparison.

The transition temperature T_c is strongly sensitive to the $\delta\varphi$ change especially for the thinner BTO barrier [see the slope of $T_c - (-\delta\varphi)$ curves in Fig. 7]. It can be clearly seen that the FE transition temperature is suppressed as the built-in field is increased for different BTO thicknesses. Usually, the TER effect is always significantly larger for thicker barrier with larger polarization.[3,5] Here, we find that a fundamental limit (which is more drastic for thinner FE barrier thickness) on the work temperature of FTJ-type or capacitor-type devices should also be simultaneously taken into account together with the FE barrier thickness or polarization value. In addition, and interestingly, since the electrocaloric effect is always the strongest close to the FE-PE transition,[62] such tuning of T_c by $\vec{E}_{bi}$ should be also considered in potential asymmetric FTJs for the room-temperature solid-state refrigeration.[27] Moreover, the fact that large tunneling current in asymmetric FTJs (Ref. 6)

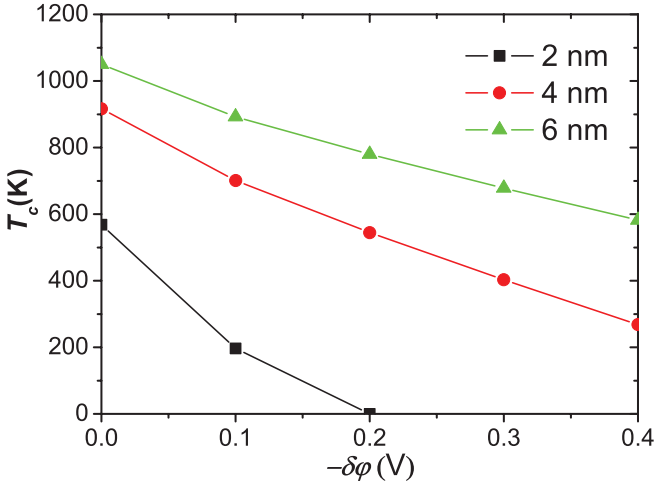

FIG. 7. (Color online) The transition temperature T_c as a function of $(-\delta\varphi)$ in epitaxial asymmetric Pt/BTO/SRO tunnel junctions with three different BTO layer thicknesses: 2, 4, and 6 nm, respectively ($E = 0$ kV/cm).

TABLE I. The different parameters extracted from Fig. 8(a).

$\delta\varphi$ (V)	$T_{\max}$ (K)	$\varepsilon_{\max+}$	$\varepsilon_{\min+}$	$\delta\varepsilon_d = (\varepsilon_{\max+} - \varepsilon_{\min+})/2$
0	1086	1001.4	24.8	513.1
−0.1	1223	428.5	23.0	225.7
−0.2	1345	285.8	21.4	153.6
−0.3	1465	218.3	20.1	119.2
−0.4	1574	178.1	18.9	98.5

results in significant Joule heating should also be included in the design of future devices.

The dielectric response ε_+ ($\vec{E}$ is parallel to $\vec{E}_{bi}$) and ε_- ($\vec{E}$ is antiparallel to $\vec{E}_{bi}$) of Pt/BTO/SRO FTJs (consider the 5-nm-thick BTO film as an example) as a function of T at different $\delta\varphi$ is shown in Figs. 8(a) and 8(b). Several key parameters with different $\delta\varphi$ in Fig. 8(a) are extracted in Table I: $T_{\max}$ corresponds to the temperature where ε_+ reaches its maximum $\varepsilon_{\max+}$; $\varepsilon_{\min+}$ simply means the minimal value of ε_+; $\delta\varepsilon_d$ is in somehow the diffuseness of the transition. It can be seen that when $\delta\varphi = 0$, ε_+ shows a sharp peak near T_c. However, a gradual decrease in $\varepsilon_{\max}$ and $\delta\varepsilon_d$ is seen upon increasing E_{bi}, which is well consistent with the results of smearing of T_c by increasing E_{bi} in Fig. 6 (see the slope of $T_c - h$ curves in Fig. 6). The diffusive transition response in ε_+ clearly shows smearing of the phase transition as a result of $\vec{E}_{bi}$, which verifies the predictions of Tagantsev *et al.*[33,34] and Bratkovsky *et al.*[44] In addition, it is shown $T_{\max}$ is shifted to higher temperatures due to $\vec{E}_{bi}$. As the strength of $\vec{E}_{bi}$ increases, the smearing of phase transition and the shift of $T_{\max}$ becomes more significant. On the other hand, the applied field can not fully compensate the built-in field, resulting in a discontinuous phase transition from the FE phase to the polar non-FE phase with temperature increasing as depicted in dielectric response ε_- in Fig. 8(b), which is distinct from the continuous counterpart of ε_+ as shown in Fig. 8(a). P_- abruptly changes its sign near the transition point resulting in a dielectric peak and a similiar smearing of ε_- by increasing the strength of $\vec{E}_{bi}$ is found. Furthermore, it is found that although the transition temperatures for two directions are different, they both decrease as the built-in field increases, which is consistent with the results without any external field (see Fig. 6), which indicates that the built-in field forces the transition to take place at a reduced temperature.

C. Comments on the built-in field effect

We make further comments on the built-in field effect in asymmetric FTJs. The main assumption in this study is that $\delta\varphi$ does not change during the polarization reversal.[33,34] The presence of $\delta\varphi$ which results in an asymmetric potential energy and barrier height differences by switching the polarization will induce the TER effect.[1–3] Note that the switching of the polarization in the asymmetric FTJs may change the value of $\delta\varphi$.[4,18,40,63,64] However, according to our analysis, the variation in $\delta\varphi$ (even changing its sign occurs during the polarization reversal) does not alter the main results of this study due to its induced broken spatial inversion symmetry of FTJs. In addition to the built-in field, if the surface term $\delta\zeta = (\zeta_2 - \zeta_1)$

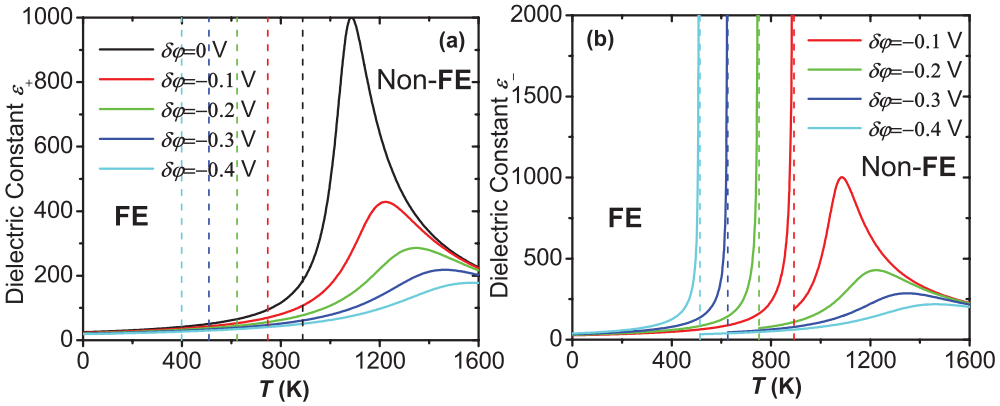

FIG. 8. (Color online) Dielectric constants ε_+ (a) and ε_- (b) as a function of temperature T at various values of $\delta\varphi$ in asymmetric Pt/BTO/SRO tunnel junctions where BTO layer thickness h is 5 nm ($E = 100$ kV/cm). The dashed lines mark the boundary between polar non-FE and FE phases for different values of $\delta\varphi$.

is nonzero, the main conclusions of this paper will not change as well.

IV. CONCLUSIONS

In summary, on the basis of a multiscale thermodynamic model, a detailed analysis of the changes brought by the built-in electric field in asymmetric FTJs is made. It is demonstrated that the critical thickness does exist in asymmetric FTJs. Below the critical thickness, it is found that there is a recovery of polar non-FE polarization due to strong canceling of the depolarizing field by the built-in field, and closurelike domains are proposed to form to minimize the system energy. It is found that the built-in electric field could not only induce imprint and a behavior of smearing of the FE phase transition, but also forces the phase transition to take place at a reduced temperature. A fundamental limit of transition temperature dependence of the barrier layer thickness on the work temperature of FTJ-type or FE-capacitor–type devices is proposed and should be simultaneously taken into account in further experiments. Hopefully, our results will be helpful to the fundamental understandings of phase transitions in asymmetric FTJs.

ACKNOWLEDGMENTS

This work is supported by the Ministry of Science and Technology of China through a 973-Project under Grant No. 2012CB619401. The authors gratefully thank X. Y. Wang, M. B. Okatan, and S. P. Alpay for their fruitful suggestions. Y. Liu is thankful to the Multidisciplinary Materials Research Center (MMRC) at Xi'an Jiaotong University for hospitality during his visit. Y. Liu and B. Dkhil wish to thank the China Scholarship Council (CSC) for funding Y.L.'s stay in France. Y. Liu, M. Bibes, and B. Dkhil also acknowledge the Agence Nationale pour la Recherche for financial support through NOMILOPS (ANR-11-BS10-016-02) project. X. J. Lou would like to thank the "One Thousand Youth Talents" program for support.

*liuyangphy52@gmail.com

[1]E. Y. Tsymbal, A. Gruverman, V. Garcia, M. Bibes, and A. Barthélémy, MRS Bull. **37**, 138 (2012).
[2]H. Kohlstedt, N. A. Pertsev, J. Rodríguez Contreras, and R. Waser, Phys. Rev. B **72**, 125341 (2005).
[3]M. Y. Zhuravlev, R. F. Sabirianov, S. S. Jaswal, and E. Y. Tsymbal, Phys. Rev. Lett. **94**, 246802 (2005).
[4]J. P. Velev, C.-G. Duan, K. D. Belashchenko, S. S. Jaswal, and E. Y. Tsymbal, Phys. Rev. Lett. **98**, 137201 (2007).
[5]V. Garcia, S. Fusil, K. Bouzehouane, S. Enouz-Vedrenne, N. D. Mathur, A. Barthélémy, and M. Bibes, Nature (London) **460**, 81 (2009).
[6]A. Gruverman, D. Wu, H. Lu, Y. Wang, H. W. Jang, C. M. Folkman, M. Y. Zhuravlev, D. Felker, M. Rzchowski, C. B. Eom, and E. Y. Tsymbal, Nano Lett. **9**, 3539 (2009).
[7]A. Crassous, V. Garcia, K. Bouzehouane, S. Fusil, A. H. G. Vlooswijk, G. Rispens, B. Noheda, M. Bibes, and A. Barthélémy, Appl. Phys. Lett. **96**, 042901 (2010).
[8]A. Chanthbouala, A. Crassous, V. Garcia, K. Bouzehouane, S. Fusil, X. Moya, J. Allibe, B. Dlubak, J. Grollier, S. Xavier, C. Deranlot, A. Moshar, R. Proksch, N. D. Mathur, M. Bibes, and A. Barthélémy, Nat. Nanotechnol. **7**, 101 (2011).
[9]D. I. Bilc, F. D. Novaes, J. Íñiguez, P. Ordejón, and P. Ghosez, ACS Nano **6**, 1473 (2012).
[10]D. Pantel, H. D. Lu, S. Goetze, P. Werner, D. J. Kim, A. Gruverman, D. Hesse, and M. Alexe, Appl. Phys. Lett. **100**, 232902 (2012).
[11]A. Chanthbouala, V. Garcia, R. O. Cherifi, K. Bouzehouane, S. Fusil, X. Moya, S. Xavier, H. Yamada, C. Deranlot, N. D. Mathur, M. Bibes, A. Barthélémy, and J. Grollier, Nat. Mater. **11**, 860 (2012).
[12]M. Y. Zhuravlev, S. S. Jaswal, E. Y. Tsymbal, and R. F. Sabirianov, Appl. Phys. Lett. **87**, 222114 (2005).
[13]C.-G. Duan, S. S. Jaswal, and E. Y. Tsymbal, Phys. Rev. Lett. **97**, 047201 (2006).
[14]S. Sahoo, S. Polisetty, C.-G. Duan, S. S. Jaswal, E. Y. Tsymbal, and C. Binek, Phys. Rev. B **76**, 092108 (2007).
[15]C.-G. Duan, Julian P. Velev, R. F. Sabirianov, W. N. Mei, S. S. Jaswal, and E. Y. Tsymbal, Appl. Phys. Lett. **92**, 122905 (2008).
[16]M. K. Niranjan, J. D. Burton, J. P. Velev, S. S. Jaswal, and E. Y. Tsymbal, Appl. Phys. Lett. **95**, 052501 (2009).
[17]J. D. Burton and E. Y. Tsymbal, Phys. Rev. B **80**, 174406 (2009).

[18] J. P. Velev, C.-G. Duan, J. D. Burton, A. Smogunov, M. K. Niranjan, E. Tosatti, S. S. Jaswal, and E. Y. Tsymbal, Nano Lett. **9**, 427 (2009).
[19] M. Y. Zhuravlev, S. Maekawa, and E. Y. Tsymbal, Phys. Rev. B **81**, 104419 (2010).
[20] V. Garcia, M. Bibes, L. Bocher, S. Valencia, F. Kronast, A. Crassous, X. Moya, S. Enouz-Vedrenne, A. Gloter, D. Imhoff, C. Deranlot, N. D. Mathur, S. Fusil, K. Bouzehouane, and A. Barthélémy, Science **327**, 1106 (2010).
[21] M. Hambe, A. Petraru, N. A. Pertsev, P. Munroe, V. Nagarajan, and H. Kohlstedt, Adv. Funct. Mater. **20**, 2436 (2010).
[22] S. Valencia, A. Crassous, L. Bocher, V. Garcia, X. Moya, R. O. Cherifi, C. Deranlot, K. Bouzehouane, S. Fusil, A. Zobelli, A. Gloter, N. D. Mathur, A. Gaupp, R. Abrudan, F. Radu, A. Barthélémy, and M. Bibes, Nat. Mater. **10**, 753 (2011).
[23] H. L. Meyerheim, F. Klimenta, A. Ernst, K. Mohseni, S. Ostanin, M. Fechner, S. Parihar, I. V. Maznichenko, I. Mertig, and J. Kirschner, Phys. Rev. Lett. **106**, 087203 (2011).
[24] L. Bocher, A. Gloter, A. Crassous, V. Garcia, K. March, A. Zobelli, S. Valencia, S. Enouz-Vedrenne, X. Moya, N. D. Marthur, C. Deranlot, S. Fusil, K. Bouzehouane, M. Bibes, A. Barthélémy, C. Colliex, and O. Stáphan, Nano Lett. **12**, 376 (2012).
[25] J. M. López-Encarnación, J. D. Burton, Evgeny Y. Tsymbal, and J. P. Velev, Nano Lett. **11**, 599 (2011).
[26] D. Pantel, S. Goetze, D. Hesse, and M. Alexe, Nat. Mater. **11**, 289 (2012).
[27] Y. Liu, X.-P. Peng, X. J. Lou, and H. Zhou, Appl. Phys. Lett. **100**, 192902 (2012).
[28] X. Luo, B. Wang, and Y. Zheng, ACS Nano **5**, 1649 (2011); H. Lu, D. J. Kim, C.-W. Bark, S. Ryu, C. B. Eom, E. Y. Tsymbal, and A. Gruverman, Nano Lett. **12**, 6289 (2012).
[29] R. R. Mehta, B. D. Silverman, and J. T. Jacobs, J. Appl. Phys. **44**, 3379 (1973).
[30] J. Junquera and P. Ghosez, Nature (London) **422**, 506 (2003).
[31] D. J. Kim, J. Y. Jo, Y. S. Kim, Y. J. Chang, J. S. Lee, J.-G. Yoon, T. K. Song, and T. W. Noh, Phys. Rev. Lett. **95**, 237602 (2005).
[32] N. A. Pertsev and H. Kohlstedt, Phys. Rev. Lett. **98**, 257603 (2007).
[33] G. Gerra, A. K. Tagantsev, and N. Setter, Phys. Rev. Lett. **98**, 207601 (2007).
[34] A. K. Tagantsev, G. Gerra, and N. Setter, Phys. Rev. B **77**, 174111 (2008).
[35] M. Stengel, D. Vanderbilt, and N. A. Spaldin, Nat. Mater. **8**, 392 (2009).
[36] Y. Zheng, W. J. Chen, C. H. Woo, and B. Wang, J. Phys. D: Appl. Phys. **44**, 139501 (2011).
[37] Y. Zheng, W. J. Chen, X. Luo, B. Wang, and C. H. Woo, Acta Mater. **60**, 1857 (2012).
[38] M.-Q. Cai, Y. Zheng, P.-W. Ma, and C. H. Woo, J. Appl. Phys. **109**, 024103 (2011).
[39] M.-Q. Cai, Y. Du, and B.-Y. Huang, Appl. Phys. Lett. **98**, 102907 (2011).
[40] Y. Umeno, J. M. Albina, B. Meyer, and C. Elsässer, Phys. Rev. B **80**, 205122 (2009).
[41] X. H. Liu, Y. Wang, P. V. Lukashev, J. D. Burton, and E. Y. Tsymbal, Phys. Rev. B **85**, 125407 (2012).
[42] H. Lu, X. Liu, J. D. Burton, C.-W. Bark, Y. Wang, Y. Zhang, D. J. Kim, A. Stamm, P. Lukashev, D. A. Felker, C. M. Folkman, P. Gao, M. S. Rzchowski, X. Q. Pan, C.-B. Eom, E. Y. Tsymbal, and A. Gruverman, Adv. Mater. **24**, 1209 (2012).
[43] J. G. Simmons, Phys. Rev. Lett. **10**, 10 (1963).
[44] A. M. Bratkovsky and A. P. Levanyuk, Phys. Rev. Lett. **94**, 107601 (2005).
[45] J. F. Scott, *Ferroelectric Memories* (Springer, Berlin, 2000).
[46] Y. Liu and X.-P. Peng, Appl. Phys. Express **5**, 011501 (2012).
[47] Y. Liu and X.-P. Peng, Chin. Phys. Lett. **29**, 057701 (2012).
[48] M. B. Okatan, I. B. Misirlioglu, and S. P. Alpay, Phys. Rev. B **82**, 094115 (2010).
[49] J. Junquera and P. Ghosez, J. Comput. Theor. Nanosci. **5**, 2071 (2008).
[50] I. I. Naumov, L. Bellaiche, and H. X. Fu, Nature (London) **432**, 737 (2004).
[51] I. Naumov and A. M. Bratkovsky, Phys. Rev. Lett. **101**, 107601 (2008).
[52] I. Kornev, H. X. Fu, and L. Bellaiche, Phys. Rev. Lett. **93**, 196104 (2004).
[53] P. Aguado-Puente and J. Junquera, Phys. Rev. Lett. **100**, 177601 (2008).
[54] T. Shimada, S. Tomoda, and T. Kitamura, Phys. Rev. B **81**, 144116 (2010).
[55] C. T. Nelson, B. Winchester, Y. Zhang, S.-J. Kim, A. Melville, C. Adamo, C. M. Folkman, S.-H. Baek, C.-B. Eom, D. G. Schlom, L.-Q. Chen, and X. Q. Pan, Nano Lett. **11**, 828 (2011).
[56] C.-L. Jia, K. W. Urban, M. Alexe, D. Hesse, and I. Vrejoiu, Science **331**, 1420 (2011).
[57] X. Y. Wang, Y. L. Wang, and R. J. Yang, Appl. Phys. Lett. **95**, 142910 (2009); Y. L. Wang, X. Y. Wang, Y. Liu, B. T. Liu, and G. S. Fu, Phys. Lett. A **374**, 4915 (2010).
[58] A. M. Bratkovsky and A. P. Levanyuk, J. Comput. Theor. Nanosci. **6**, 465 (2005).
[59] X. J. Lou and J. Wang, J. Phys.: Condens. Matter **22**, 055901 (2010).
[60] Y. S. Kim, J. Y. Jo, D. J. Kim, Y. J. Chang, J. H. Lee, T. W. Noh, T. K. Songa, J.-G. Yoon, J.-S. Chung, S. I. Baik, Y.-W. Kim, and C. U. Jung, Appl. Phys. Lett. **88**, 072909 (2006).
[61] H. Z. Jin and J. Zhu, J. Appl. Phys. **92**, 4594 (2002).
[62] J. F. Scott, Annu. Rev. Mater. Res. **41**, 229 (2011).
[63] M. Stengel, P. Aguado-Puente, N. A. Spaldin, and J. Junquera, Phys. Rev. B **83**, 235112 (2011).
[64] F. Chen and A. Klein, Phys. Rev. B **86**, 094105 (2012).
[65] We used the following set of parameters (in SI units): $u_m = -0.02458$, $Q_{12} = -0.045$, $\varepsilon_0 = 8.85 \times 10^{-12}$, $\varepsilon_b \approx 50\varepsilon_0$, $S_{11} = 8.3 \times 10^{-12}$, $S_{12} = -2.7 \times 10^{-12}$, $\eta_{\mathrm{SRO}} = 0.113$, $\eta_{\mathrm{Pt}} = 0.113$, $\lambda_{\mathrm{SRO}} = 1.2 \times 10^{-11}$, $\lambda_{\mathrm{Pt}} = 3 \times 10^{-13}$. The Landau coefficients α_i^* [the expressions can be originally found in N. A. Pertsev, A. K. Tagantsev, and N. Setter, Phys. Rev. B **61**, R825 (2000)], electrostrictive coefficients, and elastic compliances of BTO at room temperature we used are the same as those in Refs. 27, 36 and 37. The effective screening length λ_i and the coefficients of the surface energy expansion η_i are taken from Refs. 33–35, respectively. The background dielectric constant ε_b is taken from Refs. 36 and 37 which is distinct from $7\varepsilon_0$ used in Refs. 33 and 34. In fact, there is no consensus on its exact value, especially by the theoretical researchers. In this study, we have made some comparisons with the previous studies in Refs. 36 and 37, so selecting $50\varepsilon_0$ is reasonable and does not change the main results of this work. The approximated parameters in this work need more rigorous treatment by the first-principles calculations or experimental confirmation in the future.